Available online at www.garmian.edu.krd

Passer Journal of Basic and Applied Sciences

Passer 7 (Issue 2) (2025) 608-615

Original Article

Removal of Chromium (VI) and Copper (II) from Aqueous Solutions Using Biochars Derived from Wheat Straw and Wood Dust

Aram Mustafa Muhamad*[1,2] , Tariq Faruq Sadiq [1]

[1] *Department of Soil and Water, Salahaddin University, Erbil 4401, Kurdistan Region, Iraq.*
[2] *Garmian Agriculture Research Center, Sulaymaniyah 46001, Kurdistan Region, Iraq.*

Received 08 April 2025; revised 15 May 2025;
accepted 05 June 2025; available online 03 July 2025

DOI: 10.24271/psr.2025.514950.2060

ABSTRACT

Heavy metals found in water sources create dangerous environmental problems and health hazards that stem from industrial, agricultural and domestic activities. The objective of this study focused on examining biochar made from wheat straw (WSB) and wood dust (WDB) as an eco-friendly solution for extracting chromium Cr (VI) and copper Cu (II) from an aqueous solution. The biochar materials underwent pyrolysis at various temperatures between 500°C to 600°C, and their characteristics were evaluated. Freundlich, Langmuir, and Temkin isotherm were used to evaluate the WSB and WDB adsorption capacities. The results showed that WSB exhibited elevated carbon content (72%), cation exchange capacity (CEC) (44 cmol kg^{-1}), and nitrogen (N) levels (1.12%), whereas WDB demonstrated superior surface area (26.35 m^2 g^{-1}), pore radius (69.2 Å), and volatile matter (50%), highlighting the differing adsorption and nutrient characteristics of the biochars. Cr (VI) adsorption on WSB varied from 22.64 ± 0.93 to 113.37 ± 2.5 mg kg^{-1}, whereas adsorption onto WDB ranged from 21.68 ± 2.25 to 77.37 ± 0.5 mg kg^{-1}, indicating the lowest and greatest adsorption capabilities reported under the studied circumstances for each biochar. The WSB and WDB materials displayed Cu (II) adsorption variables between 47.95 ± 0.24 to 131.38 ± 0.7 mg kg^{-1} while WDB adsorbed from 48.38 ± 0.07 to 145.84 ± 0.08 mg kg^{-1} at 50 and 150 mg L^{-1} initial concentrations. The isotherm results showed that the Freundlich model is the best model for describing Cr (VI) adsorption across WSB (R^2 = 0.9771) and WDB (R^2 = 0.8439) and the Temkin model for Cu (II) adsorption in WSB (R^2 = 0.7673) but the Langmuir model for WDB (R^2 = 0.9781). WSB shows stronger adsorption for Cr (VI), while WDB is more effective for Cu (II) removal, indicating their potential for wastewater treatment applications.

Keywords: Adsorption; water treatment; heavy metals; bio sorbent; agricultural waste; isotherm models.

1 Introduction

Heavy metals in water bodies must be treated because their toxicity and non-degradability pose threats to human health and the environment [1]. Heavy metals in water bodies have been treated using a variety of methods, such as adsorption, chemical treatment, precipitation, membrane separation, flocculation, and ion exchange. Since adsorption is thought to be one of the most widespread and efficient methods, several adsorbents have been created and applied in heavy metal treatment systems [2]. Activated carbon and other conventional adsorbents [3], and silicagel [4], have a high cost of operation.

* Corresponding author
E-mail address aramzandi581@gmail.com (Instructor).
Peer-reviewed under the responsibility of the University of Garmian.

In contrast, biochar has a huge surface area, a porous structure, it is less costly and an excellent absorbent. Usually, biomass is pyrolyzed under oxygen-limited conditions to produce biochar [5]. The main purpose of biochar is to eliminate organic contaminants and heavy metals [6].
Research has proven biochar's effectiveness at immobilizing heavy metals both in water and soil and it decreases both their accessibility and movement [7,8]. According to Xiao *et al.* [9] biochar has high adsorption capacity in heavy metal removal especially in adsorption Cr (IV) and Cu (II).
Biochar produced from wheat straw has established strong Cr (VI) adsorption potential through processes that involve surface complexation while concurrently reducing Cr(VI) to the less toxic Cr (VI) [7]. According to Ali *et al.* [10]. Using wheat straw, biochar was created to study the removal of Cr (VI) from tainted water streams. With an adsorption capacity of 97%, WSB

demonstrated a remarkable level of efficacy. The adsorption capacity of wood dust biochar for Cu (II) works effectively because it possesses both strong metal-ion affinity and high cation exchange potential [11]. According to Eleryan *et al.* [12]. WDB It has good ability to remove heavy metals from water, especially Cu (II). Moreover, the utilization of agricultural waste for biochar production aligns with circular economy principles, offering a dual benefit of waste valorization and environmental protection. This research builds on the foundational work of Lehmann and Joseph [13] and Chen and Yuan [14], while advancing the understanding of biochar's role in addressing contemporary environmental challenges [11,15].

Hence, the objective of this research was intended to bridge these knowledge gaps through the examination of WSB and WDB adsorption performance when handling Cu (II) and Cr (VI) in aqueous solutions. The research studies provide information on how biochar properties including surface area porosity and pore volume measurements affect adsorption capacity.

2 Materials and methods

2. 1 Reagents and chemicals

All analytical grades have been used in this study, such as potassium dichromate ($K_2Cr_2O_7$) and copper (II) sulphate ($CuSO_4$), H_2SO_4 and NaOH were purchased from Sigma-Aldrich® and were used to prepare the standard solutions. All the solutions were prepared using distilled water.

2. 2. 1 Biochar production

The first step was preparing a machine locally to prepare to biochar based on the procedure was described by Lamichhane *et al.* [16] which is very simple to use and cost-effective. In brief, the machine consists of a double barrel a small one (35-gallon capacity) inside a large one (60-gallon capacity).

The second was collection of 100 kg of wheat residue from local farmers in the study area and wood dust in the local carpenter. Thin initial cleaning of raw materials with distilled water to get rid of any dust or residue and drying in an oven for 12 hours at 105°C using an oven (model Genlab Thermal Engineers SDO/220 Germany).

Finally, biochar production in the process of biochar production used a method that reported by Li *et al.* [17]. Subsequently, dried wheat straw (WS) and wood dust (WD) were exposed to the pyrolysis process at 500 °C in an open field for 2 h. The barrel inside was filled with biomass, undergoing pyrolysis because the barrels prevent the burning of WS and WD.

To ensure that the pyrolysis temperature was 500ºc, continuously with a laser thermometer (model UNI-T UT306S). Total process check was 24 hours from pyrolysis to cooling, and the final product was made, and then biochar was passed through 100 mesh (model, LC-dolida 100 Mesh) sieves to collect a fine fraction of WSB and WDB. This study was conducted in 2023 in the Kalar district of Sulaimani province at the Garmian Agricultural Research Center.

2.2.2 Biochar characterization

Biochar was characterized using a variety of analytical methods. The surface area was measured at 77.3 K using a Quantachrome AS1Win™, surface area analyzer (version 2.01, Quantachrome). The samples were degassed at 100°C for 9 hours before analysis. The total surface area was calculated using the multipoint Brunauer-Emmett-Teller (BET) technique, whereas pore volumes, pore radii, and interior surface areas were obtained from desorption isotherms using the Barrett-Joyner-Halenda (BJH) method [18]. Volatile matter was computed as the difference between the original weight and the weight after pyrolysis, and ash content was evaluated by heating 5 g of biochar at 700°C for 4 hours in a muffle furnace (model KSL-1000X, USA) and weighing the difference. The moisture content was determined by drying 5 g of biochar at 100°C for 10 minutes with a moisture analyzer (Ohaus model MB45, Switzerland). The Walkley-Black method, as described in Allison [19], was used to determine the total carbon content. The pH and (EC) were measured from mixing 10 grams of biochar with 100 mL of distillated water and then read pH and EC by using (ALLa pH -meter, model pH SX-610 and HANNA EC- meter model HI 98304), respectively [20]. The (CEC) was determined following the standard method (1M NH_4OAc) buffered at pH 7 as described by Samsuri *et al.* [21]. For elemental analysis, biochar samples were sieved to 1 mm and 0.25 g of biochar was digested with 2 mL of 30% H_2O_2 and 6 mL of 65% HNO_3 in a 100 mL tube, followed by heating in a hot block digester for 45 minutes, following the method of [22]. The analysis of total Nitrogen (N) was found by using the Kjeldahl method (model K-350, Germany), whereas total Phosphorus (P) and Magnesium (Mg) were measured by a (spectrophotometer model UV-9200).

2. 3 Batch adsorption experimentation

A batch study for the heavy metals Cu (II) and Cr (VI) adsorption onto the surface of either WSB or WDB was conducted with a constant pH, equilibrium time (48h), and room temperature (25 ± 2 °C), within different concentrations (0, 50, 75, 100, 125, and 150 mg/L of Cu (II) and Cr (VI) prepared in a buffer solution at a pH of 6.6). Exactly 0.2 g of Cu (II) and Cr (VI) was used as the surface of the adsorbent. Then, 40 mL of either Cu (II) or Cr (VI), at a range of concentration dosage, were transferred to the centrifuge tubes containing 0.2 g of either WSB or WDB. The centrifuge tubes were rigorously mixed on a rotary shaker for 48 h at a speed of 120 rpm (Revolutions Per Minute). The inductively coupled plasma optical emission spectroscopy **(ICP-OES)** instrument was finally used for measuring the concentrations of the Cu (II) and Cr (VI) ions. This study presented all of the data using the average of the three measurements made under each experimental condition. Control samples without biochar were included to determine the degrees of adsorption of copper and chromium from solutions without the WSB and WDB. To evaluate and compare the adsorption capacities of the WSB or WDB for Cu (II) and Cr (VI) in this study, the three widely used models, Freundlich, Langmuir, and Temkin adsorption isotherm models in linear forms, were employed to investigate Cu (II) and Cr (VI) adsorption in the studied biochar's. The Freundlich, Langmuir, and Temkin equations are presented as follows:

Langmuir Isotherm model

$$q_{ads} = \frac{b\,K_L C_e}{1+K_L\,C_e} \qquad (1)\ [23,24]$$

Where:

q_{ads} is the (Cu (II), Cr (VI)) adsorbed of biochar (mg kg^{-1}), C_e is the equilibrium (Cr (VI), Cu (II)) concentration in biochar solution (mg L^{-1}), and b and K_L = Langmuir constants; b is the maximum adsorption capacity of the biochar (mg kg^{-1}). K_L is correlated to the binding energy of (Cu (II) and Cr (VI)) to the biochar. Also, the adsorption factor (R_L) was achieved from Equation 2.

$$R_L = \frac{1}{1+K_L\,C_e} \qquad (1)\ [23,24]$$

Freundlich Isotherm model:

$$q_{ads} = K_F\,C_e^{\ 1/n} \qquad (3)\ [24]$$

Where:

q_{ads} is the (Cu (II), Cr (VI)) adsorbed of biochar (mg kg^{-1}), C_e is the equilibrium concentration of (Cu (II), Cr (VI)) in soil solution (mg L^{-1}), K_f is the proportionality constant for Freundlich model (mg kg^{-1}), and n is the empirical constant related to bonding energy biochar for (Cu (II), Cr (VI)),

Temkin Isotherm model:

$$q_{ads} = a + b\ ln\ C_e \qquad (4)\ [24]$$

Where:

q_{ads} is the (Cu (II), Cr (VI)) adsorbed of biochar (mg kg^{-1}), a is the amount of (Cu (II), Cr (VI)) b adsorbed in Temkin model (mg kg^{-1}), b is the buffer capacity of Temikn model (mL g^{-1}), and C_e is the equilibrium (Cu (II), Cr (VI)) concentration in biochar solution (mg L^{-1}).

2. 4 Statistical analysis

SPSS Statistics and Microsoft Excel 2010 software was used for calculating the coefficient of determination (R^2) and standard error (SE) to evaluate which model better described the adsorption phenomena.

3 Result and discussion

3. 1 Biochar physicochemical properties

Table (1) shows the results of the physical and chemical properties of (WDB) and (WSB). The results found considerable variations in their characteristics, which may impact their future uses in soil and water pollutant adsorption. The wheat straw biochar showed higher amounts of moisture (4.3%), pH (7.8), EC (2.3 mS cm^{-1}), CEC (44 cmol+ kg^{-1}). carbon content (72%) and total N (1.12%) compared to (WDB). The result is consistent with Ibrahim and Tariq [25]. Due to this property It makes WSB a better option for retaining nutrients and water, thereby enhancing soil fertility [13,26]. Similarly, the ash material content in WSB was higher than that in WDB. However, the ratio of (volatile Matter in WDB was higher than in WSB, which is mostly due to the difference in the source of their main source. However, WDB recorded higher pore volume (0.058 cc g^{-1}) and surface area (26.35 m^2/g), together with Potassium (K^+) (0.40%) and Calcium (Ca^{2+}) (2.4%) content. The result is consistent with Ghani *et al.* [27]. Due to its high surface area, WDB is much more suitable for adsorption uses [28,29]. In addition, both biochar's had low concentrations of heavy metals, which is another point that leads to use them safely. Concerning their properties, WSB provides excellent conditions for carbon capture and soil enrichment with nutrients, while WDB excels at contaminant fixation and features related to porosity [30].

Table 1: Selected physicochemical properties of the studied biochar's (mean=3±SE).

Parameters	**Value**		**parameters**	**Value**	
	WSB	**WDB**		**WSB**	**WDB**
Moisture (%)	4.3 ± 0.018	2.73 ± 0.015	**Total S (%)**	0.013 ± 0.0033	0.60 ± 0.25
PH	7.8 ± 0.14	7.6 ± 0.088	**Total Mg+2 (%)**	0.05 ± 0.0034	0.013 ± 0.00044
EC (ms cm^{-1})	2.3 ± 0.017	0.66 ± 0.011	**Total Cd (mgkg^{-1})**	3.74 ± 0.0023	3.62 ± 0.015
CEC (cmol kg^{-1})	44 ± 8.5	29 ± 5.5	**Total Cr (mg kg^{-1})**	1.22 ± 0.012	1.41 ± 0.0066
carbon Content (%)	72 ± 0.58	54 ± 1.73	**Total Ni (mg kg^{-1})**	4.92 ± 0.012	4.45 ± 0.014
Ash Content (%)	6.5 ± 0.29	5.7 ± 0.033	**Total Cu (mg kg^{-1})**	2.33 ± 0.015	2.22 ± 0.0088
Volatile Matter (%)	24.6 ± 0.22	50 ± 0.058	**Total Zn (mg kg^{-1})**	1.17 ± 0.0088	1.18 ± 0.066
Total N (%)	1.12 ± 0.08	0.96 ± 0.030	**Total Pb (mg kg^{-1})**	4.05 ± 0.0133	3.9 ± 0.0088
Total P (%)	0.03 ± 0.0001	0.02 ± 0.00042	**Surface area $_{BET}$ ($m^2\ g^{-1}$)**	17.672	26.35
Total K^+ (%)	0.081± 0.047	0.40 ± 0.044	**Pore volume (cc g^{-1})**	0.042	0.058
Total Na^+ (%)	0.036 ± 0.088	0.03 ± 0.0018	**Pore radius (Å)**	17.03	69.195
Total Ca^{+2} (%)	0.9 ± 0.058	2.4 ± 0.011			

3. 2 Chromium and Copper adsorption

To provide knowledge on the sorption reactions and mechanisms, sorption research is very important. Cu (II) and Cr (VI) were analyzed through Inductively Coupled Plasma Optical Emission Spectroscopy (ICP-OES). In this study, WSB and WDB have been used as adsorbent materials due to their unique characteristics, such as high surface area and functional groups (Table 1). The (CEC) of biochars has a major impact on their chemical absorption capabilities, its porosity and alkaline ash concentration make determining its (CEC) challenging, through electrostatic interactions, high CEC improves the biochar's capacity to absorb positively charged pollutants like nutrients and heavy metals, higher CEC biochars, which are usually made at lower pyrolysis temperatures and enhance cation retention, have more functional groups, CEC is required to maximize the use of biochar for environmental remediation [31]. The amount of Cu (II) and Cr (VI) adsorption on the studied biochars (WSB and WDB) is determined by subtracting the remaining amount of Cu (II) and Cr (VI) in the solution from the applied amount. Table 2 shows the adsorption of Cu (II) and Cr (VI) on each of the studied biochars at various Cu (II) and Cr (VI) concentrations and 48 hr. incubation periods. The results showed that each biochar has a distinct capacity for Cu (II) and Cr (VI) adsorption. The adsorption of Cr (VI) and Cu (II) by WSB and WDB over 48 hours varied depending on the initial metal concentration (Table 2). When the initial concentration was 50 mg L^{-1} WSB (22.64±0.93 mgL^{-1}) Cr (VI) and (47.95±0.24 mgL^{-1}) Cu (II) were removed. However, when the concentration was 150 mg L^{-1}, WSB (113.37±2.5 mgL^{-1}) Cr (VI), and (131.38±0.7 mgL^{-1}) Cu (II) was removed. At a concentration of 50 mg L^{-1}, WDB (21.68±2.25 mg L^{-1}) Cr (VI) and (48.38±0.07 mg L^{-1}) Cu (II) were removed. When the concentration was 150 mg L^{-1}, WDB (77.37±0.5 mg L^{-1}) Cr (VI) and (145.84±0.08 mg L^{-1}) Cu (II) were removed. Order adsorbed of dosage in (WSB and WDB) is as follows: (150 > 125 > 100 > 75 > 50 mg L^{-1}). In general, both WSB and WDB are effective sorbents for the removal of Cr (VI) and Cu (II). WSB exhibited better Cr (VI) adsorption capacity at elevated concentrations, yet WDB demonstrated stronger performance for Cu (II) removal when the highest concentration was applied [12,32]. With (WSB) and (WDB), the adsorption of Cu (II) and Cr (VI) increased dramatically with increasing Cr (VI) and Cu (II) content. According to Li *et al.* [33] high surface area and porosity in biochars more active sites for adsorption are made possible by this porosity. As described by Eletta *et al.* [34] biochar can more effectively physically capture and absorb metals when they are present in high quantities. It has been found that the temperature of the media in which biochar is applied also affects its adsorption capability, the majority of research revealed that the adsorption efficiency rose with temperature, indicating that the adsorption process is endothermic [32]. The scientists found that because the sorption process is endothermic, the amount of in dig carmine that sorbs onto potassium hydroxide-activated biochar increases as the temperature rises, as the temperature rises, the dye molecule's mobility increases and the adsorbent's porosity may also increase, this might possibly be because rising temperatures cause the adsorbent's internal structure to expand, allowing more dye to penetrate farther for best removal efficiency ion absorption [35]. According to Datta *et al.* [36] the solution's pH is one of the most crucial factors that greatly affects the surface charges, the adsorbent's level of ionization, and the metal ion speciation, studied heavy metals that begin to decrease at PH4 - 7. The effect of exposure time on heavy metal absorption using biochar biomass is one of the factors. Changes in biochar's adsorption capacity over time, due to interactions with pollutants, affect its effectiveness in wastewater treatment. The adsorption effectiveness of biochar drops from its original high level when it becomes saturated. Its functionality can be restored via regeneration techniques including heat or chemical treatments [37]. The sorbent-sorbate equilibrium of an adsorption system is significantly impacted by the adsorbent dose as well. According to this study, using a single dose is more effective in removing of Cr (VI) and Cu(II) ions.

Table 2: The amount of Cu (II) and Cr (VI) ions adsorbed (mg kg^{-1}) by WSB and WDB during 48 hours.

Time	**Cr (VI), Cu (II) mg L^{-1}**	**WSB (Adsorbed) mg kg^{-1} ± SE**		**WDB (Adsorbed) mg kg^{-1} ± SE**	
		Cr (VI)	**Cu (II)**	**Cr (VI)**	**Cu (II)**
48 hr	50	22.64 ± 0.93	47.95 ± 0.24	21.68 ± 2.25	48.38 ± 0.07
	75	43.86 ± 1.14	72.863 ± 0.28	27.09 ± 1.36	72.77 ± 0.08
	100	67.34 ± 0.9	97.037 ± 0.20	47.88 ± 0.36	97.3 ± 0.05
	125	91.1 ± 1.6	108.33 ± 2.05	62.68 ± 3.3	122 ± 0.06
	150	113.37 ± 2.5	131.38 ± 0.7	77.37 ± 0.5	145.84 ± 0.08

3. 3 Adsorption isotherms

The values of the adsorption isotherm parameters are displayed in Table (3) after the isotherm adsorption data were fitted to the Freundlich, Langmuir, and Temkin adsorption models. The results explained that all three adsorption models were fit for all adsorption data. However, the Cr (VI) adsorption behavior of WSB followed the Freundlich model with R^2 0.9771 n 0.19 and Kf 1.55 mg kg^{-1} , WDB's Cr (VI) adsorption followed the Freundlich model with an R^2 value of 0.8439, an n value of 0.73, and a Kf value of 5 mg kg^{-1}. Cr (VI) adsorption in WSB and WDB followed the Freundlich model. While the Cu (II) adsorption fitted poorly for all models (Freundlich R^2 = 0.6889). WDB biochar achieved better Cu (II) adsorption than WSB which was best explained by the Langmuir model with an R^2 value of 0.9781 b value of -322 mg kg^{-1} and KL value of -0.086 mg L^{-1}. An n value of 0.73 and a Kf value of 5 mg kg^{-1}. Biochar's displayed reasonable Temkin isotherm fits with R^2 values between 0.9335 and 0.9707 and different AT and BT (A_T: Temkin isotherms equilibrium binding constant L g^{-1}, B_T: Temkin constant related to the heat of adsorption). Values in Figures (1a-d) through (3a-d). The different adsorption mechanisms support that Cr (VI) adsorption shows heterogeneous behavior (Freundlich) yet Cu (II) adsorption on WDB follows Langmuir's monolayer mechanism because of their distinct metal-binding capacities. The result agrees with Romar-Gasalla *et al.* [32] who found that the Freundlich model was the best fitted for Cr (VI) adsorption WSB. Furthermore Sirusbakht *et al.* [35] studied Cr (VI) fixation and found that the Freundlich model described Cr (VI) adsorption very well in the WDB. These assumptions can be further verified based on the adsorption of Cr and Cu in WSB and WDB on the points of Figure (1a-d) for the Freundlich plots, and Figures (2a-d, 3a-d) for the Langmuir and Temkin plots.

Table 3: Fitting parameters for the kinetics of Cu (II) and Cr (VI) adsorption on WSB and WDB biochars.

Biochar	Element	Time (hr)	Freundlich Isotherm			Langmuir Isotherm				Temkin Isotherm		
			n	Kf (mg kg^{-1})	R^2	b (mg kg^{-1})	KL (mg L^{-1})	RL	R^2	AT (mg L^{-1})	BT	R^2
WSB	Cr (VI)	48	0.19	1.55	0.9771	-11	-0.025	-3.8-0.36	0.9601	0.039	8.5	0.9335
	Cu (II)		3.9	58	0.6889	145	0.50	0.013-0.039	0.7152	15	112	0.7673
WDB	Cr (VI)		0.73	5	0.8439	-189	-0.004	1.22-2.15	0.8263	0.046	43	0.7957
	Cu (II)		0.83	7	0.9636	-322	-0.086	-0.084-0.30	0.9781	0.99	23	0.9707

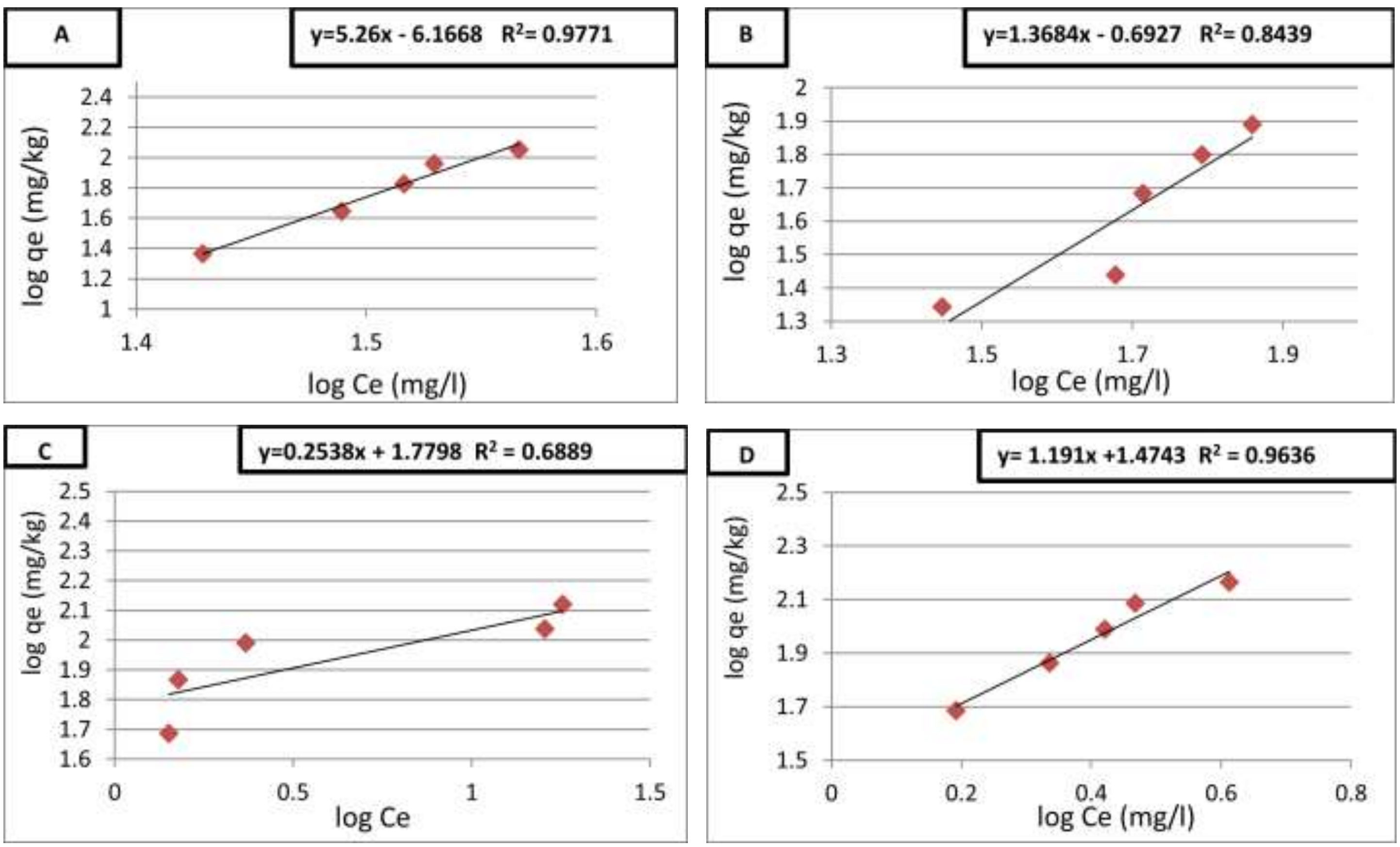

Figure 1: Linear form of Freunlich adsorption isotherm. (a) adsorption Cr (VI) by WSB, (b) adsorption Cr (VI) by WDB, (c) adsorption Cu (II) by WSB, (d) adsorption Cu (II) by WDB.

The Langmuir model is widely used in surface chemistry, catalysis, and environmental engineering, especially for describing adsorption on solid surfaces. However, it doesn't account for certain factors, like interactions between adsorbate molecules, and may not apply well to more complex adsorption systems (such as multilayer adsorption) [38]. As shown in Table (3), the KL values were different between the two biochars, and the importance of KL indicates the extent of the spontaneous adsorption reaction. The larger the K value, the greater the spontaneity and the more sustainable the yields, leading to a weaker supply of Cu (II) and Cr (VI). The result is in agrees with Eleryan *et al.* [12] is similar who found that the Langmuir model is the best fit for Cu adsorption in the studied WDB and Figure (2), which suggests favorable conditions for the adsorption of Cr and Cu, in the case of Langmuir.

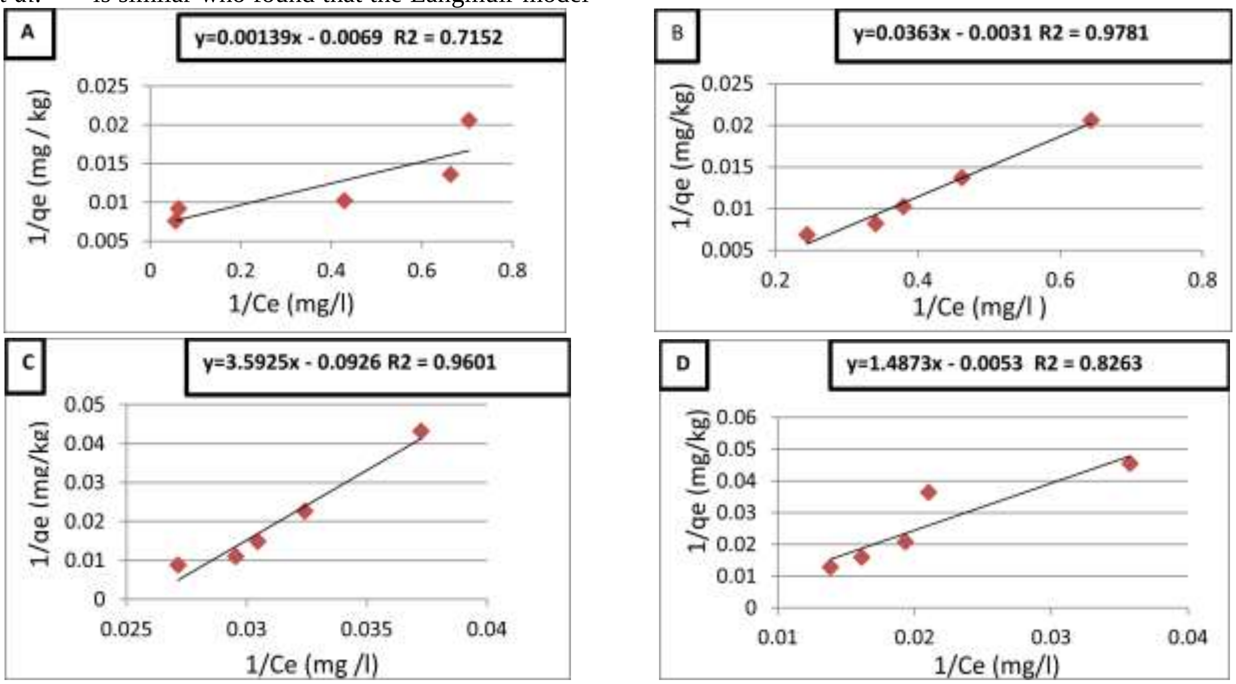

Figure 2: Linear form of Longmuir adsorption isotherm. (a) adsorption Cu (II) by WSB, (b) adsorption Cu (II) by WDB, (c) adsorption Cr (VI)by WSB, (d) adsorption Cr (VI)by WDB.

The Temkin model assumes that the heat of the adsorption reduces linearly with coverage (multilayer process) [39]. Figure (3) shows the Tamkin models that refer to the adsorption process of Cu (II) and Cr (VI) ions to WSB and WDB. Although the results indicated that the Timkin model was the best fit in WSB and to describe the adsorption of Cu (II). However, this result does not agree with Wang *et al.* [23] which argues that the Langmuir model is more appropriate for the Cu (II) adsorption process in WSB than the Freundlich and Temkin models because the Langmuir model accurately captures the saturation of adsorption sites as Cu (II) concentration increases.

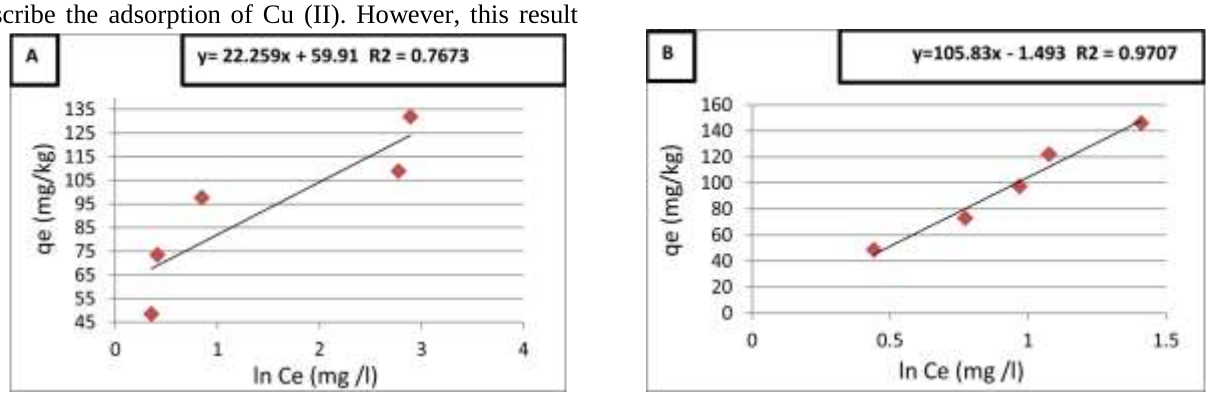

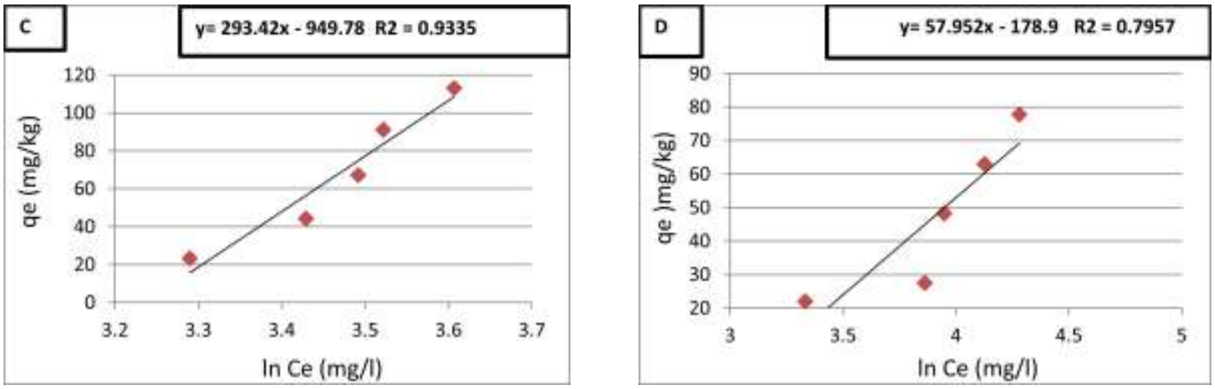

Figure 3: Linear form of Temkin adsorption isotherm. (a) adsorption Cu (II) by WSB, (b) adsorption Cu (II) by WDB, (c) adsorption Cr (VI) by WSB, (d) adsorption Cr (VI) by WDB.

Conclusion

The results showed that (WSB) and (WDB) have distinct physicochemical properties, leading to different adsorption behaviors. WDB exhibited a higher adsorption capacity due to its greater surface area and larger pore size compared to WSB. However, WSB demonstrated stronger Cr (VI) adsorption capacity, attributed to its higher carbon content and (CEC), which supports multilayer adsorption as described by the Freundlich model. Surface charge development and ion exchange processes appeared to influence ash content differently in the two biochar's, with WSB having a higher ash content than WDB. Both biochar samples exhibited slightly alkaline pH values. The total elemental compositions, particularly (Ca^{2+}), (K^{+}) and (Na^{+}) varied between the two types. WDB contained higher levels of (Ca^{2+}) and (K^{+}) while (Na^{+}) content was also greater in WDB compared to WSB. Environmental applications work best when the selection of biochar occurs through the evaluation of its physical and chemical properties for better removal of heavy metals. In addition, studies need to examine alternative methods of biochar conversion that enhance adsorption performance, especially for the removal of pollutants in wastewater treatment facilities.

Availability of data

The article contains all of the data generated or analyzed during this study.

Conflicts of Interest

The authors of this research state that they have no conflicts of interest with regard to its publication.

Acknowledgment

The authors thank the Soil and Water Laboratory at Garmian Agricultural Research Center for their laboratory support.

References

[1] Rajput, S., Pittman Jr, C. U. & Mohan, D. Magnetic magnetite (Fe3O4) nanoparticle synthesis and applications for lead (Pb2+) and chromium (Cr6+) removal from water. *J. Colloid Interface Sci* **468**, 334-346 (2016).

[2] Ifthikar, J., Wang, J., Wang, Q., Wang, T., Wang, H., Khan, A., Jawad, A., Sun, T., Jiao, X. & Chen, Z. Highly efficient lead distribution by magnetic sewage sludge biochar: sorption mechanisms and bench applications. *Bioresour. Technol* **238**, 399-406 (2017).

[3] Bohli, T., Ouederni, A., Fiol, N. & Villaescusa, I. Evaluation of an activated carbon from olive stones used as an adsorbent for heavy metal removal from aqueous phases. *C. R. Chim* **18**, 88-99 (2015).

[4] Najafi, M., Yousefi, Y. & Rafati, A. Synthesis, characterization and adsorption studies of several heavy metal ions on amino-functionalized silica nano hollow sphere and silica gel. *Sep. Purif. Technol* **85**, 193-205 (2012).

[5] Tang, Q., Dai, W., Niu, J., Wang, J., Yin, W., Yan, X., Jiang, Y., Cheng, Y., Wang, S. & Wang, X. Straw and Biochar Amendments Over a Decade Differently Modulates Denitrification Gas Products. *Water Air Soil Pollut* **235**, 773 (2024).

[6] Syarifuddin, S., Heryanto, H., Suryani, S. & Tahir, D. Biochar from diverse wastes: A comprehensive bibliometric analysis of heavymetal adsorption in wastewater. *Desalin. Water Treat* **317**, 100089 (2024).

[7] Deng, T., Li, H., Ding, S., Chen, F., Fu, J. & Zhao, J. Enhanced Adsorptivity of Hexavalent Chromium in Aqueous Solutions Using CTS@ nZVI Modified Wheat Straw-Derived Porous Carbon. *Nanomaterials* **14**, 973 (2024).

[8] Dun, Y., Wu, C., Zhou, M., Tian, X. & Wu, G. Wheat straw-and maize straw-derived biochar effects on the soil cadmium fractions and bioaccumulation in the wheat–maize rotation system. *Front. Environ. Sci* **10**, 980893 (2022).

[9] Xiao, F., Cheng, J., Cao, W., Yang, C., Chen, J. & Luo, Z. Removal of heavy metals from aqueous solution using chitosan-combined magnetic biochars. *J. Colloid Interface Sci* **540**, 579-584 (2019).

[10] Ali, S., Noureen, S., Shakoor, M. B., Haroon, M. Y., Rizwan, M., Jilani, A., Arif, M. S. & Khalil, U. Comparative evaluation of wheat straw and press mud biochars for Cr (VI) elimination from contaminated aqueous solution. *Environ. Technol. Innov* **19**, 101017 (2020).

[11] Domingues, R. R., Trugilho, P. F., Silva, C. A., Melo, I. C. N. d., Melo, L. C., Magriotis, Z. M. & Sánchez-Monedero, M. A. Properties of biochar derived from wood and high-nutrient biomasses with the aim of agronomic and environmental benefits. *PloS one* **12**, e0176884 (2017).

[12] Eleryan, A., Aigbe, U. O., Ukhurebor, K. E., Onyancha, R. B., Eldeeb, T. M., El-Nemr, M. A., Hassaan, M. A., Ragab, S., Osibote, O. A. & Kusuma, H. S. Copper (II) ion removal by chemically and

physically modified sawdust biochar. *Biomass Convers. Biorefin* **14**, 9283-9320 (2024).
[13] Lehmann, J. & Joseph, S. *Biochar for environmental management: science, technology and implementation*. (Taylor & Francis, 2024).
[14] Chen, B. & Yuan, M. Enhanced sorption of polycyclic aromatic hydrocarbons by soil amended with biochar. *J. Soils Sediments* **11**, 62-71 (2011).
[15] Shi, X., Yang, W., Li, J. & Yao, Z. The Application of Biochar as Heavy Metals Adsorbent: The Preparation, Mechanism, and Perspectives. *Int. J. Environ. Res* **18**, 41 (2024).
[16] Lamichhane, B., Dunn, B. & Singh, H. Preparation of biochar for use as a soil amendment. (Oklahoma Cooperative Extension Service, 2023).
[17] Li, Y., Xing, B., Ding, Y., Han, X. & Wang, S. A critical review of the production and advanced utilization of biochar via selective pyrolysis of lignocellulosic biomass. *Bioresour. Technol* **312**, 123614 (2020).
[18] Samsuri, A., Sadegh-Zadeh, F. & Seh-Bardan, B. Characterization of biochars produced from oil palm and rice husks and their adsorption capacities for heavy metals. *Int. J. Environ. Sci. Technol* **11**, 967-976 (2014).
[19] Allison, L. Organic carbon. *Methods of soil analysis: Part 2 Chem. Microbiol. Prop* **9**, 1367-1378 (1965).
[20] Samsuri, A., Tariq, F., Karam, D., Aris, A. & Jamilu, G. The effects of rice husk ashes and inorganic fertilizers application rates on the phytoremediation of gold mine tailings by vetiver grass. *Appl. Geochem* **108**, 104366 (2019).
[21] Samsuri, A., Tariq, F., Karam, D., Aris, A. & Jamilu, G. Distribution of heavy metals fractionation in gold mine tailing amended with non-coated and iron-coated rice husk ash. *Soil Sediment Contam* **30**, 532-547 (2021).
[22] Tariq, F., Samsuri, A., Karam, D. & Aris, A. Phytoremediation of Gold Mine Tailings Amended with Iron-Coated and Uncoated Rice Husk Ash by Vetiver Grass (Vetiveria zizanioides (Linn.) Nash). *Appl. Environ* **2016**, 4151898 (2016).
[23] Wang, Y., Zheng, K., Jiao, Z., Zhan, W., Ge, S., Ning, S., Fang, S. & Ruan, X. Simultaneous removal of Cu2+, Cd2+ and Pb2+ by modified wheat straw biochar from aqueous solution: preparation, characterization and adsorption mechanism. *Toxics* **10**, 316 (2022).
[24] Tariq, F., Abdulrahman, C. & Rasheed, M. in IOP Conf. Ser.: Earth Environ. Sci 012016 (IOP Publishing).
[25] Ibrahim, L. F. & Tariq, F. Production and Comparison of biochar derived from slow pyrolysis and ash from burnt of wheat straw residue. *Zanco J. Pure Appl. Sci* **35** (2023).
[26] Tsai, W.-T., Liu, S.-C., Chen, H.-R., Chang, Y.-M. & Tsai, Y.-L. Textural and chemical properties of swine-manure-derived biochar pertinent to its potential use as a soil amendment. *Chemosphere* **89**, 198-203 (2012).
[27] Ghani, W. A. W. A. K., Mohd, A., da Silva, G., Bachmann, R. T., Taufiq-Yap, Y. H., Rashid, U. & Al-Muhtaseb, A. a. H. Biochar production from waste rubber-wood-sawdust and its potential use in C sequestration: chemical and physical characterization. *Ind. Crops Prod* **44**, 18-24 (2013).
[28] Khan, H. A., Naqvi, S. R., Mehran, M. T., Khoja, A. H., Niazi, M. B. K., Juchelková, D. & Atabani, A. A performance evaluation study of nano-biochar as a potential slow-release nano-fertilizer from wheat straw residue for sustainable agriculture. *Chemosphere* **285**, 131382 (2021).
[29] Taherymoosavi, S., Joseph, S., Pace, B. & Munroe, P. A comparison between the characteristics of single-and mixed-feedstock biochars generated from wheat straw and basalt. *J. Anal. Appl. Pyrolysis* **129**, 123-133 (2018).
[30] Tehreem, S., Yousra, M., Alamer, K. H., Alsudays, I. M., Sarwar, S., Kamal, A. & Naeem, S. Analysis of the role of various biochar in the remediation of heavy metals in contaminated water and its kinetics study. *J. Saudi Chem. Soc* **26**, 101518 (2022).
[31] Munera-Echeverri, J. L., Martinsen, V., Strand, L. T., Zivanovic, V., Cornelissen, G. & Mulder, J. Cation exchange capacity of biochar: An urgent method modification. *Sci. Total Environ* **642**, 190-197 (2018).
[32] Romar-Gasalla, A., Coelho, G. F., Nóvoa-Muñoz, J. C., Arias-Estévez, M., Fernández-Sanjurjo, M. J., Álvarez-Rodríguez, E. & Núñez-Delgado, A. Wheat straw as a bio-sorbent for arsenate, chromate, fluoride, and nickel. *Water* **9**, 690 (2017).
[33] Li, H., Dong, X., da Silva, E. B., de Oliveira, L. M., Chen, Y. & Ma, L. Q. Mechanisms of metal sorption by biochars: Biochar characteristics and modifications. *Chemosphere* **178**, 466-478 (2017).
[34] Eletta, O. A., Adeniyi, A. G., Ighalo, J. O., Onifade, D. V. & Ayandele, F. O. Valorisation of Cocoa (Theobroma cacao) pod husk as precursors for the production of adsorbents for water treatment. *Environ. Technol. Rev* **9**, 20-36 (2020).
[35] Sirusbakht, S., Vafajoo, L., Soltani, S. & Habibi, S. Sawdust bio sorption of chromium (VI) ions from aqueous solutions. *Chem. Eng* **70** (2018).
[36] Datta, D., Gehlot, G., Singh, G., Bhardwaj, A. & Kumar, D. Removal of malachite green, a cationic textile dye using Amberlite polymeric resins. *Indian Chem. Eng* **63**, 339-348 (2021).
[37] Ighalo, J. O., Adeniyi, A. G., Eletta, O. A. & Arowoyele, L. T. Competitive adsorption of Pb (II), Cu (II), Fe (II) and Zn (II) from aqueous media using biochar from oil palm (Elaeis guineensis) fibers: a kinetic and equilibrium study. *Indian Chem* **63**, 501-511 (2021).
[38] Yu, B., Zhang, Y., Shukla, A., Shukla, S. S. & Dorris, K. L. The removal of heavy metal from aqueous solutions by sawdust adsorption—removal of copper. *J. Hazard. Mater* **80**, 33-42 (2000).
[39] Majd, M. M., Kordzadeh-Kermani, V., Ghalandari, V., Askari, A. & Sillanpää, M. Adsorption isotherm models: A comprehensive and systematic review (2010− 2020). *Sci. Total Environ* **812**, 151334 (2022).